

See discussions, stats, and author profiles for this publication at: <https://www.researchgate.net/publication/6673494>

Degenerate Electron Exchange Reaction of n – Alkane Radical Cations in Solution

ARTICLE *in* THE JOURNAL OF PHYSICAL CHEMISTRY A · DECEMBER 2006

Impact Factor: 2.69 · DOI: 10.1021/jp0638944 · Source: PubMed

CITATIONS

5

READS

32

5 AUTHORS, INCLUDING:



Vsevolod I Borovkov

Russian Academy of Sciences

61 PUBLICATIONS 353 CITATIONS

SEE PROFILE



Nina Gritsan

Russian Academy of Sciences

168 PUBLICATIONS 2,055 CITATIONS

SEE PROFILE



V. A. Bagryansky

Russian Academy of Sciences

51 PUBLICATIONS 391 CITATIONS

SEE PROFILE



Yuri N. Molin

Russian Academy of Sciences

258 PUBLICATIONS 2,171 CITATIONS

SEE PROFILE

Degenerate Electron Exchange Reaction of *n*-Alkane Radical Cations in Solution

Vsevolod I. Borovkov,^{*,†,‡} Nina P. Gritsan,^{†,‡} Iliya V. Yeletskikh,[‡] Viktor A. Bagryansky,^{†,‡} and Yuri N. Molin[†]

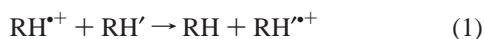
Institute of Chemical Kinetics and Combustion of SB RAS, ul. Institutskaya, 3, Novosibirsk 630090, Russia, and Novosibirsk State University, ul. Pirogova, 2, Novosibirsk 630090, Russia

Received: June 21, 2006; In Final Form: September 22, 2006

The degenerate electron exchange (DEE) reaction involving radical cations (RCs) of *n*-nonane, *n*-dodecane, and *n*-hexadecane in *n*-hexane solution was studied over the temperature range 253–313 K using the method of time-resolved magnetic field effect in recombination fluorescence of spin-correlated radical ion pairs. In the dilute solutions the rate constant of DEE was found to be 200 times slower than the diffusion limit. Using *n*-nonane as an example, we showed that two reasons are responsible for the low value of the RC self-exchange rate: (1) conformational variability of molecules and RCs and (2) the activation barrier of DEE reaction. The calculations of the reaction enthalpy performed by the B3LYP/6-31G(d) method indicated that electron transfer can be effective only upon collision of RC with a neutral molecule either in the all-trans conformation or in the conformation differing from the latter by rotation of the end ethyl fragment. The activation barrier of the DEE reaction was estimated using the reorganization energy of the internal degrees of freedom calculated at the B3LYP level and was found to be about 6 kcal/mol. A possible influence of the interaction between RC and a neutral molecule in an encounter complex on DEE rate constant is also discussed.

I. Introduction

Solvent radical cations (RCs) arising upon ionizing irradiation of alkane solutions are the primary carriers of the positive charge. The measurements of the conductivity of irradiated alkane solutions demonstrated that the rate of solvent RC transport depends drastically on the alkane structure.^{1–5} Thus, in cyclohexane and a series of other cycloalkanes, the mobility of solvent RCs (holes) is 1–2 orders of magnitude as high as that of molecular ions in these cycloalkanes.^{2–4} Such a high mobility was attributed to a fast degenerate electron exchange (DEE) involving solvent holes:



On the other hand, in *n*-alkanes no substantial differences in the mobility of solvent holes and molecular radical ions were observed.⁴ That is why no information about the DEE rate involving *n*-alkane RCs has been obtained by measuring solution conductivity.

As compared with the conductivity technique, the ESR method allows measuring lower rates of DEE. The exchange manifests itself in broadening and collapse of ESR lines due to the jumping of unpaired electron from one magnetic nuclei environment to another.^{6–8} However, the conventional ESR method is not sensitive enough to detect alkane RCs in solution. With a more sensitive technique, optically detected ESR,^{9–11} the exchange narrowed ESR line of *n*-pentadecane RC was observed in solution and the DEE rate constant was estimated.¹²

Additional possibilities for measuring the DEE rate of radical ions are provided by the method of time-resolved magnetic field effect (TR MFE) in the recombination fluorescence of spin-correlated radical ion pairs.^{13–15} This method has been recently

used to detect RCs of several *n*-alkanes in the octane–hexadecane series in *n*-hexane solutions.¹⁶ The ESR spectra widths for *n*-alkanes RCs in solution measured in these experiments were found to be smaller than that recorded in low-temperature matrixes. This was attributed to the averaging of hyperfine coupling (HFC) constants in RC due to fast conformational transitions in RC and the rotation of methyl groups. It has also been observed that increasing the concentration of the *n*-alkanes causes further narrowing of the ESR spectra that was explained qualitatively in terms of the DEE involving *n*-alkane RC. Estimations indicated that in the case of *n*-nonane RC the DEE rate constant was about 2 orders of magnitude as low as that of diffusional encounters of RC with *n*-nonane molecules in *n*-hexane.¹⁶

In the present work the TR MFE method was applied to measure the rates of degenerate electron exchange involving RCs of *n*-nonane (C9), *n*-dodecane (C12), and *n*-hexadecane (C16) in *n*-hexane solutions over the temperature range of 253–313 K. The density functional calculations were used to estimate the factors determining the DEE rate constant in the cases under study.

II. Experimental and Computational Details

Materials and Methods. *n*-Hexane (99%), *n*-octane, *n*-nonane, *n*-dodecane, and *n*-hexadecane (98%, “Reactiv”, Russia) were stirred with concentrated sulfuric acid, washed with water, and dried over CaCl₂. *n*-Hexane, *n*-octane, and *n*-nonane were additionally distilled and then passed repeatedly through a 1 m column of activated alumina and stored over sodium. Using gas chromatography, we found that in the case of *n*-hexane the used treatment failed to remove 2-methylpentane and 3-methylpentane that were the main impurities and amounted to 0.2% and 0.5%, respectively. Other impurities (up to 0.05%) were not identified. The main impurities in *n*-alkanes used as solutes were found to be their branched isomers in concentrations of 1–2%.

* Corresponding author. E-mail: borovkov@kinetics.nsc.ru.

[†] Institute of Chemical Kinetics and Combustion of SB RAS.

[‡] Novosibirsk State University.

We assume that the presence of these isomers has no significant effect on our results. *p*-Terphenyl-*d*₁₄ (*p*-TP, Aldrich, 98%) was used as received. The solutions were degassed by repeated freeze–pump–thaw cycles. The temperature during measurements was stabilized within ± 1 K.

The delayed fluorescence decays of *n*-alkane solutions were detected by the single photon counting technique using the homemade X-ray fluorometer described elsewhere.¹⁷ The repetition frequency of ionizing pulses with a quantum energy of about 20 keV was 80 kHz. The duration of the pulses was about 2 ns and the apparatus response function was close to Gaussian with fwhm of about 2.5 ns. When an experimental TR MFE curve was obtained, the typical value of the irradiation dose absorbed by the sample was no more than 10 krad, and no effects of the dose accumulation were observed. The light was collected using an optical band-pass filter (260–390 nm). To decrease the influence of instrumental drift, the fluorescence decays were registered for periods of 250 s, alternatively, with and without external magnetic field. Zero magnetic field was adjusted to within ± 0.05 mT, the strength of high magnetic field was 0.1 T.

Quantum Chemical Calculations. The geometries of *n*-alkanes and their radical cations in various conformations of the electronic ground states were fully optimized by the density functional theory at the hybrid B3LYP level^{18,19} with the 6-31G(d) basis set using the Gaussian 98 suite of programs.²⁰ This approach was also used to calculate reorganization energies for the degenerate electron transfer in the case of cyclohexane radical cation (vide infra). The HFC constants were calculated at the same level of theory. The free energies of solvation of different conformations of C9 molecule and RC were calculated using the polarized continuum model (PCM or Tomashi model^{21,22}) as implemented in Gaussian 98. Calculations were performed for the nonpolar solvent (*n*-heptane) whose properties are similar to those used in our experiments. The geometries of *n*-nonane RC in the all-trans conformation were also optimized taking into account solvent in the PCM model and at the UMP2/6-31G(d) level.

Spin Dynamics Calculations. The recombination fluorescence kinetics in a nonpolar solvent can be expressed as²³

$$I(t) \approx \tau_{\text{fl}}^{-1} \int_0^t F(t') \left[\theta \rho_{\text{ss}}(t') + \frac{1}{4}(1 - \theta) \right] \exp(-(t - t')/\tau_{\text{fl}}) dt' \quad (2)$$

where $F(t)$ is the recombination rate of radical ion pairs, which is assumed to be the same for both spin-correlated and noncorrelated radical ion pairs,²⁴ and θ is the fraction of pairs formed in the singlet-correlated state.^{10,23} The function $\rho_{\text{ss}}(t)$ describes the population of the singlet spin state of these pairs and τ_{fl} is the lifetime of the singlet-excited states of luminophore. In a real experiment the observed fluorescence kinetics is the convolution of (2) with the apparatus response function.

The time-resolved magnetic field effect is the $I_{\text{B}}(t)/I_0(t)$ ratio of the kinetic curves of the recombination fluorescence decay of irradiated solutions with and without magnetic field, respectively. Within the limit of a short fluorescence time, τ_{fl} , this ratio is independent of the recombination kinetics, $F(t)$, and is determined by the spin evolution of radical pairs.

In the absence of paramagnetic relaxation and significant difference in the g -values of radicals involved, the $\rho_{\text{ss}}^{\text{B},0}(t)$ functions can be written as^{7,15}

$$\rho_{\text{ss}}^{\text{B}}(t) = \frac{1}{2} + \frac{1}{2} G_{\text{c}}^{\text{B}}(t) G_{\text{a}}^{\text{B}}(t) \quad (3)$$

$$\rho_{\text{ss}}^0(t) = \frac{1}{4} + \frac{3}{4} G_{\text{c}}^0(t) G_{\text{a}}^0(t) \quad (4)$$

The $G(t)$ functions are determined by the characteristics of the radical anion or RC that is marked by indices *a* and *c*, respectively. In the case of unresolved ESR spectrum of a radical, the $G(t)$ function can be determined in the quasi-classical approximation:⁷

$$G^{\text{B}}(t) = \exp[-(\gamma\sigma t^2/2)] \quad (5)$$

$$G^0(t) = \frac{1}{3} [1 + 2(1 - (\gamma\sigma t)^2) \exp[-(\gamma\sigma t)^2/2]] \quad (6)$$

where σ^2 is the second moment of the ESR spectrum of the corresponding radical and γ is the gyromagnetic ratio for a free electron.

Equations 3–6 were derived for the case of the absence of any radical ion reactions. If any radical ion participates in DEE, one should take into account a random change in the projections of nuclear spins in the radical. It is known⁶ that in the limiting cases of slow ($\sigma^2\tau^2 \gg 1$) and fast ($\sigma^2\tau^2 \ll 1$) spectral exchange it can be taken into account as paramagnetic relaxation whose rate is expressed by simple dependences in terms of the reaction rate (1). In the case of an arbitrary DEE rate the $\rho_{\text{ss}}(t)$ functions can be calculated numerically.⁷ According to ref 7, for DEE involving RC, the $G_{\text{c}}^{\text{B},0}(t)$ functions should be substituted for the functions $\Gamma_{\text{c}}^{\text{B},0}(t)$ determined by the equation

$$\Gamma_{\text{c}}(t) = \sum_{n=1}^{n=\infty} G_{\text{c}}^{(n)}(t) \quad (7)$$

$$G_{\text{c}}^{(n)}(t) = \tau^{-1} \int_0^t G_{\text{c}}^{(1)}(t') G_{\text{c}}^{(n-1)}(t - t') dt'$$

is the term corresponding to the contribution of the random realization of ($n - 1$) acts of self-exchange by the time t , τ is the meantime between electron jumps, and $G_{\text{c}}^{(1)}(t) = G_{\text{c}}(t) \exp(-t/\tau)$.

Needless to say, substantial contribution to paramagnetic relaxation can be made not only by DEE but also by other mechanisms. The latter were taken into account using an approximate description of paramagnetic relaxation,^{15,23} which gives

$$\rho_{\text{ss}}^{\text{B}}(t) = \frac{1}{4} + \frac{1}{4} \exp(-t/T_1) + \frac{1}{2} \exp(-t/T_2) \Gamma_{\text{c}}^{\text{B}}(t) G_{\text{a}}^{\text{B}}(t) \quad (8)$$

$$\rho_{\text{ss}}^0(t) = \frac{1}{4} + \frac{3}{4} \exp(-t/T_0) \Gamma_{\text{c}}^0(t) G_{\text{a}}^0(t) \quad (9)$$

Here $1/T_1 = 1/T_{1\text{a}} + 1/T_{1\text{c}}$ and $1/T_2 = 1/T_{2\text{a}} + 1/T_{2\text{c}}$ are the sums of the rates of spin–lattice and phase relaxations determined by other (not related to DEE) mechanisms in high magnetic field and $1/T_0$ is the total rate of the additional phase relaxation of radical ion pair in zero field.

III. Experimental Results

Figure 1 shows the experimental TR MFE curves obtained for *n*-hexane solutions of C9 whose concentration varies from 0.07 to 3 M. In addition, the magnetic field effect is shown which has been obtained in neat *n*-nonane. In all cases the concentration of *p*-TP was low enough (3×10^{-5} M) to avoid scavenging of alkane radical cations by this solute within the time range under study. As shown earlier,¹⁶ under these

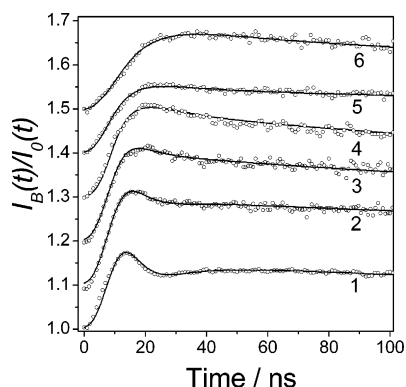


Figure 1. Experimental (scatter plots) and calculated (solid lines) curves of magnetic field effect obtained in hexane solutions of C9 with a concentration of 0.07 M (curve 1), 0.3 M (2), 0.6 M (3), 1 M (4), and 3 M (5). Curve 6 is the magnetic field effect obtained in neat *n*-nonane. In all cases the *p*TP concentration was 3×10^{-5} M. Solid lines are the results of modeling with parameters σ_c , T_1 , T_2 , T_0 and θ given in Table 1 and exchange rates adjusted for different concentrations of added C9. For convenience, the curves are shifted vertically.

TABLE 1: DEE Rate Constant, k , for *n*-alkane RCs in *n*-hexane at 293 K, and the Parameters Used To Model the Time-Resolved Magnetic Field Effect in Figure 1^a

<i>n</i> -alkane	$10^{-8}k$, $\pm 15\%$, ^b $M^{-1} s^{-1}$	σ_c , $\pm 10\%$, mT	$T_2 = T_0$, $\pm 15\%$, ns	T_1 , $\pm 25\%$, ns	θ , $\pm 10\%$
C9	2.6	0.69	18	$5 \cdot 10^2$	0.16
C12	1.6	0.40	30	$5 \cdot 10^2$	0.20
C16	2.8 (2.3) ^c	0.29	40	$6 \cdot 10^2$	0.22

^a The notation is described in the text. ^b For C16 solutions the spread in values is $\pm 20\%$. ^c For C16 solutions in *n*-octane.

conditions solvent holes generated by the ionizing pulse are captured by the molecules of added alkane with the rate, which is controlled by diffusion, that is within about 1 ns even at the lowest concentration used. On the other hand, excess electrons are captured by the *p*-TP molecules only and hence the observed delayed fluorescence originates from the recombination of ion pairs (C9)⁺/(*p*-TP)⁻. Therefore, the TR MFE curves reflect the spin evolution in the spin-correlated part of these pairs. The main contribution to the evolution is made by hyperfine interactions in RC because the HFC constants in the radical anion of perdeuterated terphenyl are low.^{15,16} As shown earlier,¹⁶ the position of TR MFE curve maximum in time is in inverse proportion to the σ value of ESR spectrum of a RC. The observed shift of the maximum with increasing C9 concentration (Figure 1) is the result of the narrowing of the ESR spectrum of C9 RC due to the increasing DEE rate in reaction 1.^{7,16}

Solid lines in Figure 1 give the calculated TR MFE curves obtained with eqs 2–9 using the parameters summarized in Table 1 (except exchange rates shown in Figure 2 for various concentrations of added *n*-alkanes). To fit the experimental curves, the main optimization parameters were the values of electron self-exchange time, τ_c , of the second moment of the ESR spectrum for RC, σ_c , the times of paramagnetic relaxation T_1 and $T_2 = T_0$, and parameter θ . For the second moment of the ESR spectrum of the *p*-TP radical anion and the lifetime of the ¹*p*-TP* singlet excited state, we used the known values $\sigma_a = 0.068$ mT¹⁵ and $\tau_{fl} = 1$ ns.²⁵

For the recombination kinetics of ion pairs in eq 2 we took the function²⁶

$$F(t) \sim (t + t_0)^{-3/2} \quad (10)$$

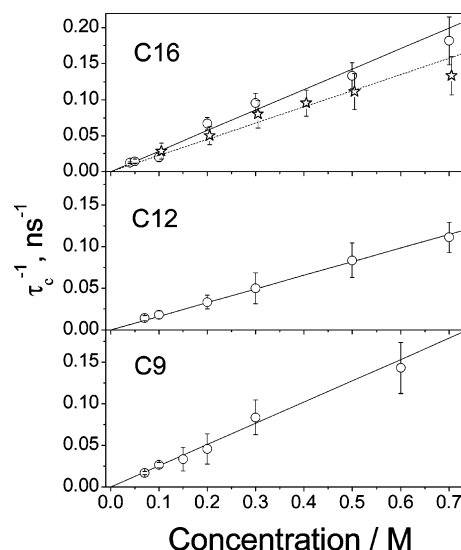


Figure 2. Optimum values of the inverse time of DEE for C9, C12, and C16 in *n*-hexane depending on concentration. Straight lines are the best linear approximations corresponding to the rate constants given in Table 1. For C16 also shown is the dependence of the rate of reaction 1 in *n*-octane (stars) and the corresponding approximation (dashed line).

The best agreement between the experimental and model kinetics was observed for t_0 values varying over the range 3–5 ns depending on the added alkane and its concentration. In any case, a 2–3-fold change in t_0 had a negligible effect on the calculated TR MFE curves except for an initial portion of the curves within several nanoseconds where the geminate recombination rate of the radical ion pairs decreases sharply by 1–2 orders of magnitude. The use of other functions often applied for approximating geminate recombination kinetics instead of (10) (see, e.g., ref 26) had no noticeable effect on the results obtained from the fitting. The reason for this is a rather short fluorescence lifetime of ¹*p*-TP* (of about 1 ns). In this case the convolution (2) is very close to the product of $F(t)$ and singlet state population probability. Therefore, the ratio of the intensities $I_B(t)/I_0(t)$ is mostly determined by spin dynamics not by $F(t)$.

Table 1 summarizes the average values of T_1 , T_2 and θ , obtained by fitting the experimental curves. When particular curves were modeled, the values of these parameters were allowed to vary within the ranges indicated in Table 1. The σ_c value was chosen and fixed so as to obtain satisfactory agreement with experiment over the entire range of used concentrations. Note that a more rigorous fitting procedure, which takes into account the recombination kinetics, has provided somewhat higher values of σ_c as compared with ref 16.

The only parameter varying over a wide range upon the fitting of TR MFE curves at various concentrations of added *n*-alkane was the electron self-exchange time, τ_c . The dependences of the values of the exchange rate, $1/\tau_c$, corresponding to the best fit, on the concentration of C9, C12, and C16 in *n*-hexane are shown in Figure 2.

For C16, Figure 2 also presents the data obtained using *n*-octane as the solvent. The ionization potential of octane is high enough as compared with that of C16. Therefore it is possible to assume that the rate of C16 RC formation is close to the diffusion-controlled limit. The straight lines in Figure 2 are the best linear fit of the experimental data over the indicated concentration range. As the concentration of the *n*-alkane increases further, the dependences deviate from linearity to a slower one.

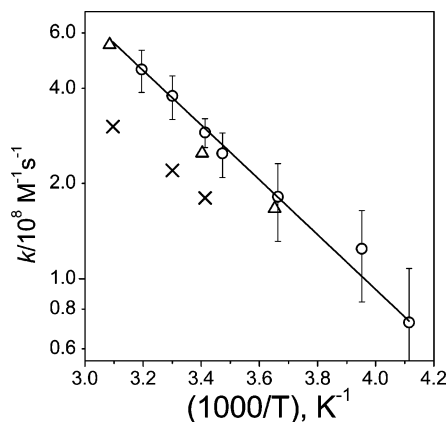


Figure 3. Arrhenius plots of DEE rate constant for C9 (○), C12 (×) and C16 (Δ) in hexane solutions. The straight line is the best approximation for C9 with the activation energy of 3.8 kcal/mol and the preexponent $2.1 \times 10^{11} \text{ M}^{-1} \text{ s}^{-1}$.

The DEE rate constants in dilute solutions were determined from the slope of the straight lines shown in Figure 2 and their values at room temperature are summarized in Table 1. For all RCs studied, the rate constants at room temperature were close to $2 \times 10^8 \text{ M}^{-1} \text{ s}^{-1}$, which was in agreement with the previous estimations.¹⁶

Figure 3 shows the Arrhenius plots of the DEE rate constants for RCs of C9, C12, and C16. For *n*-nonane the experimental points are well described by the Arrhenius dependence with the activation energy of $3.8 \pm 0.8 \text{ kcal/mol}$ and the preexponential factor of $(2.1 \pm 0.8) \times 10^{11} \text{ M}^{-1} \text{ s}^{-1}$. Although the rate constants in the case of C12 and C16 are determined over a more narrow temperature range, it is seen that similar values of the activation energy of reaction 1 hold for these cases as well.

As the temperature decreased further, TR MFE curves for C12 and C16 solutions altered, especially at high concentrations $>1 \text{ M}$, so that it was impossible to describe them using eqs 2–9. In these conditions the peak in TR MFE curves did not move to longer times and its amplitude decreased with increasing concentration of the *n*-alkane added. This phenomenon requires further investigation.

IV. Calculations

To analyze the aforementioned experimental results, one should keep in mind that the molecules of normal alkanes exist in solutions as a set of various conformations. Transitions between them take place on a subnanosecond time scale.^{27–31} It is evident that a similar situation is to be expected for RCs of *n*-alkanes.

Note that a change in a particle conformation is accompanied by a change in its energy. Thus the rate constant of electron transfer from a molecule to RC should depend on conformations in which they are upon encounter. Besides, the various conformations of RC display different distributions of spin density (vide infra). Therefore, the transitions between RC conformations are sure to have an effect on the observed spin dynamics of the radical pair involved.

Thus, a further analysis requires determining the relative fractions of different conformations for both neutral molecules and RCs in solution. Because the number of possible conformations increases drastically with increasing length of the carbon skeleton, the most detailed study of the conformation assortment was performed for the shortest alkane, i.e., *n*-nonane.

Thermodynamic Characteristics. Figure 4 shows the geometry of several conformations of C9 RC formed by rotation of the fragments of all-trans structure **I** about different C–C bonds. These conformations correspond to local minima at the potential energy surface (PES). The figure shows also the calculated HFC constants with protons in these conformations.

Structure **II** was obtained by rotation through approximately 120° about the $\text{C}_2\text{--C}_3$ bond, structure **III** by rotation about the $\text{C}_4\text{--C}_5$ bond, and structure **IV** from rotation of terminal fragments through approximately 120° in opposite directions about the $\text{C}_3\text{--C}_4$ and $\text{C}_6\text{--C}_7$ bonds. The calculations demonstrate that the bond lengths and the bond angles in the optimized geometry of molecules differ slightly from the corresponding values for RC. However, for at least a small number of turned fragments the local minima at PES correspond to similar structures. It is worth noting that the free energies of solvation (of about 19.4 kcal/mol) were found to be very similar for different conformations.

Table 2 summarizes some of the calculated thermodynamic characteristics of C9 conformers shown in Figure 4. It also includes characteristics for C12 and C16. Note that the calculated gas-phase vertical ionization potentials obtained for C9 and C12 are in fair agreement with the experimental gas-phase IPs.^{32–34} Besides, the values of the increase in the formation enthalpy of the conformations of both the neutral molecule and radical cation of C9 in comparison with the all-trans conformation of the corresponding species are included. Table 2 presents also the reorganization energy of the internal degrees of freedom of reagents in reaction 1 in the high-temperature limit ($\lambda_{\text{in}}^\infty$) calculated for RC and molecule in all-trans conformations. These values were calculated as follows

$$\lambda_{\text{in}}^\infty = E_{\text{n-eq}}(\text{B}^+) - E_{\text{eq}}(\text{B}^+) + E_{\text{n-eq}}(\text{B}) - E_{\text{eq}}(\text{B}) \quad (11)$$

where $E_{\text{n-eq}}(\text{B}^+)$ is the electronic energy of RC with the geometry optimized for the molecule, $E_{\text{eq}}(\text{B}^+)$ is RC electronic energy in the equilibrium geometry, $E_{\text{n-eq}}(\text{B})$ is the electronic energy of the molecule with the geometry optimized for RC, and $E_{\text{eq}}(\text{B})$ is the molecule electronic energy in the equilibrium geometry. The values of $\lambda_{\text{in}}^\infty$ will be used below to estimate the activation energy barrier of DEE.

Conformations of Neutral Molecules. To estimate the relative amounts of different conformations for the neutral molecules of C9, we used the Boltzmann distribution. Because the total number of C9 molecule conformations is large enough,²⁷ the formation enthalpy was calculated only for several selected conformers with a large number of rotations about C–C bonds. The UB3LYP/6-31G(d) method predicts that the characteristic increase in the formation enthalpy of the C9 conformer with respect to structure **I** is about 0.8–0.9 kcal/mol per every rotation about a C–C bond. These values exceed the experimental values (0.5–0.6 kcal/mol) estimated from the Raman spectra in the series nonane–eicosane.³⁵ To eliminate the disagreement between the calculated and experimental values, one should apply high-level ab initio calculations as shown for *n*-butane and *n*-hexane.²⁸

Because of this, to analyze the conformational manifold of neutral molecules we use the results of ref 31, according to which the relative conformer energy can be calculated by the formula

$$E = n_{\text{G}}\Delta E_{\text{G}} + n_{\text{G-}}\Delta E_{\text{AGD}} + n_{\text{G+}}\Delta E_{\text{AGS}} \quad (12)$$

where n_{G} , $n_{\text{G+}}$, and $n_{\text{G-}}$ are the numbers of all rotations about C–C bonds counting from the all-trans conformation, the pairs

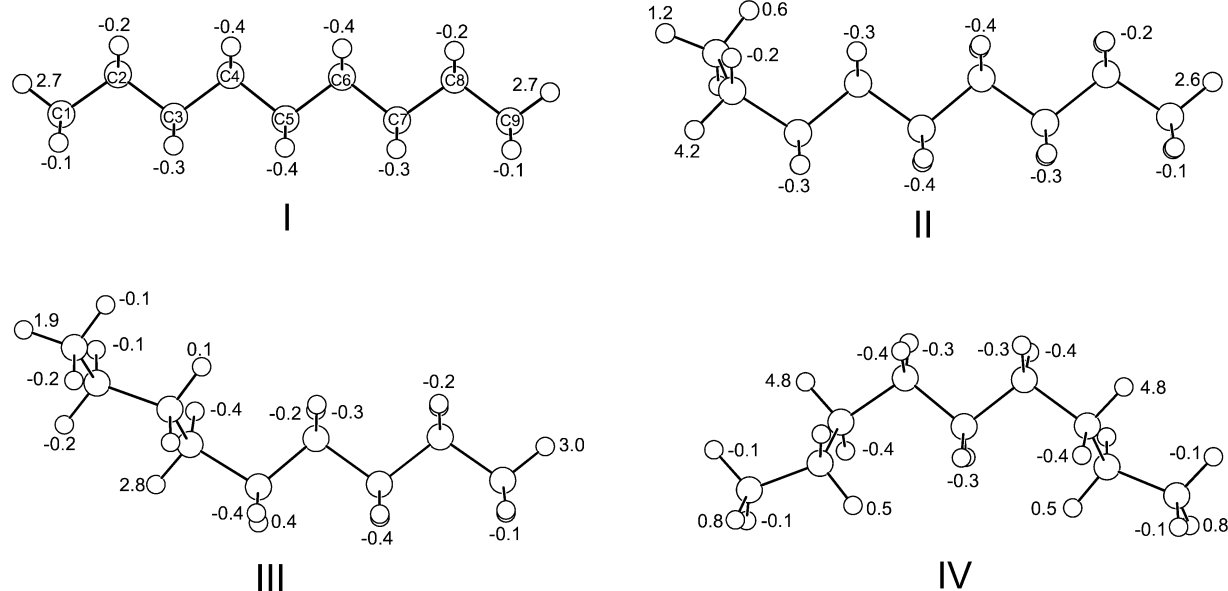


Figure 4. Conformations of *n*-nonane RC formed by rotation of fragments of the initial all-trans structure (**I**) about different C–C bonds. Structure **II** was obtained by rotation through an angle of about 120° about the C₂–C₃ bond, structure **III** is about the C₄–C₅ bond, and structure **IV** results from rotations of the end fragments through about 120° in the opposite directions about the C₃–C₄ and C₆–C₇ bonds. The figure shows HFC constants with protons in millitesla calculated by the UB3LYP/6-31G(d) method.

TABLE 2: Calculated Gas Phase Vertical (IP_v) and Adiabatic (IP_a) Ionization Potentials of *n*-Alkane Molecules for Different Conformations, the High-Temperature Limit of the Inner Reorganization Energy (λ_{in}^{∞}) for the Encounter Complex of RC and Molecule in Their All-Trans Conformations, and the Increase in the Formation Enthalpy of the Conformations of *n*-Alkane Molecules (ΔH_{molec}) and RCs (ΔH_{RC}) in *n*-Heptane As Compared to All-Trans Conformations (Conformations in Figure 4)

<i>n</i> -alkane (conformation)	IP _v , eV	IP _a , eV	λ_{in}^{∞} , eV	$\Delta(H_{molec})$, kcal/mol	$\Delta(H_{RC})$, kcal/mol
C9 (all-trans, I)	9.71 ^a	9.13	1.21	0	0
C9 (II)	9.72	9.17		0.83	1.02
C9 (III)	9.83	9.26		0.85	4.26
C9 (IV)	9.97	9.39		1.8	6.56
C12 (all-trans)	9.33 ^b	8.88	0.95		
C16 (all-trans)	9.01	8.66	0.73		

^a Experimental values of gas phase IP_v for C9 are 9.72 eV³² and 9.62 eV.³³ ^b Experimental values of gas phase IP_v for C12 is 9.43 eV.³⁴

of rotations about the neighboring bonds in the same and in the opposite directions, respectively. E is the total energy relative to the all-trans conformation, $\Delta E_G = 0.52$ kcal/mole, $\Delta E_{AGD} = 1.56$ kcal/mol, and $\Delta E_{AGS} = -0.26$ kcal/mol. These values were obtained for *n*-alkanes longer than *n*-octane by the high-level ab initio calculations.³¹

The number N of conformations with the given parameters (n_G , n_{G+} , and n_{G-}) were evaluated according to ref 27

$$N = 2^{(n_G - n_{G+} - n_{G-})} C_{n_G - 1}^{(n_G - n_{G+} - n_{G-} - 1)} C_{N_C - 2 - n_G}^{(n_G - n_{G+} - n_{G-})} C_{n_{G+} + n_{G-}}^{n_G} \quad (13)$$

where $C_a^b = a! / [(a - b)!b!]$, N_C is the number of carbon atoms in the chain. The mean number of conformations with a given number of rotations, n_G , was obtained by summing up eq 13 over all possible values of n_{G+} , $n_{G-} \geq 0$ so that $(n_{G+} + n_{G-}) < n_G$ with the weight of $\exp(-E/RT)$.

The results obtained for $n_G \leq 6$ at 293 K are summarized in Table 3. As the temperature increases from 253 to 313 K, the fraction of C9 molecules with structure **I** varies from 4.9% to

TABLE 3: Fractions of the Conformations of *n*-Alkane Molecules and C9 RC Differing in the Number of Rotations n_G about C–C Bonds As Calculated from Eqs 12 and 13

n_G	C9	C9 ⁺	C12	C16
0	3.6%	57%	0.7%	0.1%
1	17%	42%	5%	0.8%
2	32%	<0.1%	15%	3.6%
3	30%	0	25%	10%
4	15%	0	27%	18%
5	3.6%	0	18%	23%

3.1%. Note that the fraction of C9 molecules with structure **II** accounts for one-third of the total number of molecules with $n_G = 1$, i.e., about 6% at room temperature. According to the aforementioned calculations, the mean number of rotations about C–C bonds for C9 is about 2.5, which is close to 2.1 obtained by extrapolating the data of ref 29 on the average number of trans–gauche rotations at 298 K.

Conformations of Radical Cations. Our calculations predict a greater increase in the formation enthalpy of RC conformers as compared with the corresponding conformers of neutral molecules (Table 3). For the C9 RC two lower energy structures **I** and **II** predominate in solution at room temperature and their fractions amount to 57% and 41%, respectively. Upon transitions to other RC conformations, particularly to those formed by rotations about several C–C bonds, the formation enthalpy increases so much that their presence in the solution can be neglected. Even if our calculation overestimates the relative enthalpy of conformers of RC as it takes place in the case of neutral molecules of *n*-alkanes, we believe that the difference does not exceed a fraction of kcal/mol; i.e., it does not affect the above conclusion.

In the present work the conformation composition of the radical cations of C12 and C16 was not analyzed in detail. Nevertheless, as in the case of C9, it is likely that these RCs mainly exist in conformations with no more than 1 trans–gauche rotation relative to the all-trans structure.

Estimation of HFC Constants and ESR Spectrum Width for *n*-Alkane RC. As demonstrated in Figure 4, for the all-trans conformation **I** the maximum HFC constants correspond to the interaction between the electron spin and the protons of

methyl groups that are in the plane of the carbon skeleton. In the case of conformations **II**–**IV** with relatively long planar carbon skeleton, the interaction between the unpaired electron and the protons lying in the same plane is also stronger. This is in agreement with the previous results.^{36–38}

Thus, the transitions between RC conformations will cause a substantial change in HFC constants with protons. Consequently, to estimate the second moment of the ESR spectrum (σ^2) in solution (in the absence of DEE), one should average the calculated HFC constants in RC over all accessible conformations.

We performed theoretical estimation of σ^2 only for C9 RC. First of all, we took into account rotational averaging of HFC constants with the protons of the methyl groups. The activation energy of this rotation in alkane RCs is close to that for neutral molecules and amounts to 2–3 kcal/mol.^{39,40} At room temperature this leads to a high frequency of HFC constants modulation and satisfies the condition for fast spectral exchange ($\gamma\Delta\tau_c)^2 \ll 1$.⁶ $\Delta \sim 2$ mT is the characteristic value of the constants modulation in C9 RC, τ_c is the rotation correlation time and γ is the gyromagnetic ratio for free electron. In this case the protons of methyl groups are equivalent and HFC constants are a simple average over these methyl protons.

It is reasonable to assume that the characteristic times of conformational transitions in RCs and molecules are also comparable. At room temperature, the conformational relaxation time of *n*-hexane molecules (in *n*-hexane) is about 30 ps, and in the case of C16 (in liquid *n*-hexadecane) this time increases to 700 ps.^{29,30} Most probably, the relaxation slows down mostly due to an increase in hydrocarbon viscosity, because for a free molecule the transition barrier is expected to weakly depend on the hydrocarbon chain length. Even if the conformational transitions in the radical cations of C9–C16 in *n*-hexane are slower by an order of magnitude than those in hexane molecules (30 ps), this is enough for the fast spectral exchange approximation to be valid over the entire temperature range.

The high rate of spectral exchange allows applying a simplified procedure for calculating average HFC constants in RCs. After averaging the HFC constants with the protons of methyl groups for each RC conformation, we next average HFC constants with all other protons over various conformations with a weight proportional to the factor $\exp(-\Delta H/RT)$, where ΔH is the relative formation enthalpy of the given conformation. As follows from Table 2, the averaging was actually performed over conformations **I** and **II**. Using this procedure we estimated $\sigma_c \approx 1.0$ mT for C9 RC.

To verify the accuracy of the calculations, the experimental HFC constants in glassy matrixes at 77 K^{36–38} were compared with the calculated HFC constants with the protons lying in the plane of the carbon skeleton in the all-trans conformations of radical cations of a series of *n*-alkanes from pentane to decane. The calculated and experimental HFC constants are shown in Figure 5. This demonstrates that the UB3LYP/6-31G(d) calculations reproduce well the dependence of HFC constants on the number of carbon atoms. However, in all cases, the calculated values exceed the experimental ones by 0.6–0.9 mT. Therefore, in the case of low HFC constants, e.g., for RC of C9, the calculation gave 1.5-fold higher constants. The geometry of this RC calculated by the UMP2 method provided only a slight improvement (overestimation by a factor of 1.4). At the same time, calculating HFC constants by the UMP2 method, we obtained a 1.7-fold underestimation. The use of the EPR–II basis set, recommended for the calculations of HFC constants,^{41,42} led to even worse disagreement (a 1.8-fold overes-

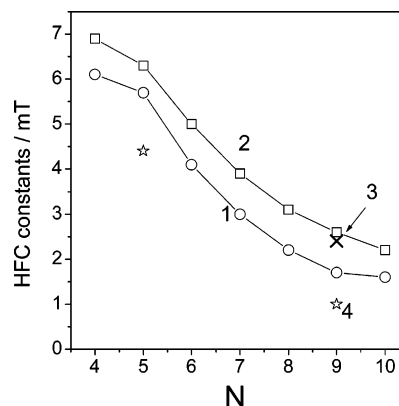


Figure 5. Experimental dependence of HFC constants for the all-trans geometry with methyl in-plane protons on the hydrocarbon (C_NH_{N+2}) chain length N (curve 1) and the same dependence predicted by UB3LYP/6-31G(d) calculations (curve 2). Cross 3 shows the B3LYP/6-31G(d) prediction at the geometry optimized by UMP2/6-31G(d) and stars 4 correspond to HFC constant predicted at UMP2/6-31G(d) level.

timization in the case of UB3LYP calculations). The account for the solvent (heptane) using the PCM model^{21,22} was found to reduce the HFC constants with the protons lying in the plane of the carbon skeleton by 8%.

V. Discussion

Theoretical Estimation of the ESR Spectrum Width. As mentioned above, UB3LYP/6-31G(d) calculations provide 1.5-fold overestimations of HFC constants with in-plane protons of C9 RC (Figure 5). It is reasonable to assume that the same overestimation also occurs in calculations of HFC constants with all other protons in all C9 RC conformations. If the calculated $\sigma_c = 1.0$ mT is reduced by a factor of 1.5, the resulting theoretical estimate will be 0.67 mT, which is in good agreement with the experimental value $\sigma_c \approx 0.69$ mT. Therefore, the results of our calculations additionally support the statement that the observed TR MFE curves are determined by HFC in *n*-alkane RCs.

As the carbon chain of RC is lengthened, the ESR spectrum width measured in low-temperature matrixes decreases.^{36–38} Therefore, in solution, the ESR spectrum width of the radical cations of C12 and C16 should be smaller than that for C9, as it was observed in our experiments.

Factors Determining the DEE Rate. The DEE rate constants presented in Table 1 are substantially lower than the diffusion limit in *n*-hexane which amounts to about $4 \times 10^{10} \text{ M}^{-1} \text{ s}^{-1}$.⁴³ It is easy to suggest several reasons for the DEE rate constant decrease. First of all, these reasons include the existence of high enough activation barrier due to the reorganization of both the medium and the internal degrees of freedom of the reagents, as well as the possible steric limitations. Besides, in the case of *n*-alkanes, there is an additional factor arising from the conformational distribution of molecules in solution.

The experimental results obtained indicate that in the DEE reaction involving *n*-alkane RCs, several factors could be equally important. This is indicated by a decrease in DEE rate with increasing solution viscosity despite the fact that the observed rate constant is 2 orders of magnitude lower than the diffusion limit. For example, the rate of DEE for C16 decreases by approximately 20% upon going from *n*-hexane to *n*-octane whose viscosity is 1.8 times higher. In addition, the rate of reaction 1 increases sublinearly with added alkane concentration when the latter exceeds 1 M. For such concentrations, the solution viscosity increases in proportion to the molar fraction

of the more viscous solute.⁴⁴ On the other hand, the activation energy of the DEE process is higher as compared with the activation energy of radical ion diffusion in *n*-hexane, which is about 2 kcal/mol.⁴⁵

We shall discuss the possible reasons for the low exchange rate constant starting with those for which we can readily perform quantitative estimations. As before, we shall consider mainly the case of C9.

Conformational Variability of *n*-Alkane Molecules. As mentioned above, the radical cation of C9 is most likely to be present in conformations **I** and **II**, because of the dramatic increase in the formation enthalpy of RC on going to more complicated conformers in contrast to the neutral molecules. The increase also results in the great disadvantage for electron transfer from C9 molecule in conformations different from these two conformations. Thus we assume the electron transfer to be efficient only when the neutral molecule involved in the reaction 1 is in one of the conformations **I** or **II**.

For simplicity, let us assume that electron transfer occurs with the probability close to unity upon encounter of RC with a molecule in any combination of conformations **I** and **II**. Besides, we assume that the lifetime of the encounter complex "RC/molecule" is short enough to prevent the change in the reagent conformations. The latter is likely to hold true for *n*-hexane solutions assuming that the time of the encounter is determined only by reagent diffusion. Indeed, taking the reaction radius $R \approx 0.7$ nm,⁴³ the reaction zone width $\delta = 0.1$ nm,⁴⁶ and the sum of reagent diffusion coefficients in *n*-hexane $D \approx 5 \times 10^{-5}$ cm²/s,^{43,47} we get the encounter time $\Delta t = \delta R/D \approx 15$ ps.⁴⁶ As mentioned in the previous section, the characteristic time of conformational transitions is either comparable to or higher than this value.

In the suggested approximation the probability of electron transfer upon the encounter of RC with a molecule in solution is determined by the fraction of structures **I** or **II** among neutral C9 molecules, which at $T = 293$ K is about $(0.036 + 0.06) \approx 0.1$. When the electron transfer probability at contact is high, one should also take into account that only half of the collisions lead to charge exchange.

Thus, the manifold of conformations of C9 molecules existing in solution is likely to lead to slowing down of reaction 1 by a factor of 20 as compared to diffusion-controlled one. Note that this estimate was obtained by neglecting the interaction of reagents that can increase the lifetime of the collision complex "RC/molecule".

Activation Energy of Electron Transfer. Obviously, even with favorable conformations of reagents, the rate constant of reaction 1 can decrease substantially due to the activation barrier related to the reorganization of both the medium and the internal degrees of freedom. The activation energy (E_a) of the degenerate electron exchange was estimated using the known result of electron transfer theory:^{48–50}

$$E_a = (\lambda_{in} + \lambda_s)/4 - V \quad (14)$$

where λ_{in} is the reorganization energy of the internal degrees of freedom, λ_s is the reorganization energy of the solvent, and V is the interaction matrix element. As an estimate for λ_s we use the value 0.15 eV, determined experimentally for electron transfer from biphenyl radical anion to a series of acceptors in bridged systems in isooctane.⁴⁸

The value of λ_{in} can be estimated as described in ref 50

$$\lambda_{in}(T) = \lambda_{in}^{\infty} \left[\frac{4k_B T}{h\nu_{in}} \tanh \frac{h\nu_{in}}{4k_B T} \right] \quad (15)$$

where λ_{in}^{∞} is the high-temperature limit of the reorganization energy (11), ν_{in} is the effective oscillation frequency of the degrees of freedom involved in reorganization, and T is temperature.

In the case of degenerate electron transfer between a C9 molecule and a C9 RC in conformation **I**, λ_{in}^{∞} is calculated by the B3LYP/6-31G* method to be 1.21 eV. As the effective frequency ν_{in} we take the characteristic frequency of C–C stretch which, according to our calculations, is about 3×10^{13} s^{–1} for both C9 and C9 RC. Therefore, at $T = 293$ K we get $\lambda_{in} = 0.9$ eV. The value of the matrix element V is assumed to be high enough for the electron transfer to be considered adiabatic, but at the same time to be insufficient to have a substantial effect on E_a value (14). In this case, $E_a \approx 6$ kcal/mol and assuming the time of contact $\Delta t \approx 15$ ps, the probability of electron transfer upon the encounter of the molecule with RC in the all-trans conformations would be $\Delta t \nu_{in} \exp(-E_a/RT) \approx 0.015$.

Role of Reagent Interaction. If both factors discussed in the previous sections operate according to the estimations and do so independently, the resulting rate constant would be several times lower than the experimental one. Besides, an additional factor capable of decreasing the DEE rate at contact is the relative orientation of the reagents, which are strongly anisotropic. It is quite probable that at some contacts the condition of reaction adiabaticity is not fulfilled. This factor decreasing the electron transfer rate can be hardly analyzed quantitatively. In any case, it supports the conclusion that electron transfer observed in the experiment is likely to be faster than expected from the simple estimations.

Note that a similar problem is even more pronounced in the attempts to quantitatively interpret DEE involving RCs of cyclic alkanes.⁴ For instance, in dilute *n*-hexane solutions of norbornane⁵¹ the DEE rate constant for norbornane RC corresponds to diffusion-controlled limit. Earlier rather fast DEE in dilute solutions was observed for RC of *cis*-decalin.⁵² Larger DEE rate constants as compared with *n*-alkanes could be attributed to the fact that both the molecule and RC of cycloalkanes have only one conformation. We performed the calculation of the reorganization energy of the internal degrees of freedom during DEE for cyclohexane radical cation, which exhibits the highest rate of DEE in liquid solution. The calculation, performed in the same manner as for *n*-alkanes, gave $\lambda_{in}^{\infty} = 1.15$ eV, which is in agreement with previously reported results on this subject.⁵³ Using the calculated effective frequency $\nu_{in} = 2.6 \times 10^{13}$ s^{–1}, we have obtained the activation barrier $E_a = 5.6$ kcal/mol, which should result in a substantial decrease in the electron-transfer rate.

We believe that the contribution of the thermal activation of electron transfer to reducing the transfer probability is overestimated in our model. The reason for this might be the longer lifetime of the encounter complex "RC/molecule" as compared to that estimated from the free diffusion model. Turning back to the previous estimation of electron-transfer probability in the encounter complex, one can note that this probability $\Delta t \nu_{in} \exp(-E_a/RT)$ increases with increasing the lifetime of the complex Δt . To achieve an agreement between the estimation and the experiment, it is sufficient to increase the lifetime of the encounter complex by less than an order of magnitude. This

can be provided by a relatively small, e.g., about 1.5 kcal/mol, value of the formation enthalpy of the complex "RC/molecule". Note that the existence of this interaction should also cause a decrease in the estimated activation energy as compared to E_a calculated with $V = 0$; see eq 14.

On our opinion, the above disagreement between the experiment and the results of simple estimations of DEE rate constant could be treated as an indirect evidence for the interaction of reagents in encounter complex "RC/molecule", which makes longer the lifetime of this complex. Unfortunately, there is no direct evidence in the literature for a feasible formation of complexes involving alkane RC.

Other *n*-Alkanes. Estimations using the results of quantum chemical calculations of reorganization energies in all-trans conformations (Table 2) give the activation energies of DEE involving C12 and C16 RCs of about 4.9 and 4.0 kcal/mole, respectively. Thus the role of the activation barrier in these cases should be of less importance as compared to C9 RC. On the other hand, the probability to find the molecule in conformations of types I or II upon transition from C9 to C12 and especially to C16 decreases substantially. It is obvious that these two factors act in opposite directions and can partially compensate each other.

VI. Conclusions

Our DFT calculations demonstrate that *n*-nonane RC is likely to be mostly either in the all-trans conformation or in a conformation differing from it by the rotation of the end ethyl fragment. The ESR spectrum widths of the *n*-alkane RCs in solution estimated using the results of UB3LYP calculations and assumption of the fast conformational transitions and the rotation of methyl groups are in fair agreement with experiment.

The concentration dependence of TR MFE curves is satisfactorily described in the assumption of the degenerate electron exchange involving the RC of the studied *n*-alkanes with a rate constant, which is 2 orders of magnitude lower than the diffusion-controlled limit. Two factors could be important in the reduction of the DEE rate constant: the noticeable activation energy of the electron transfer and the conformational variability of *n*-alkane molecules in solution.

Acknowledgment. The work was supported by the Russian Foundation for Basic Research (grant 05-03-32620) and the program of Leading Scientific Schools (NS-5078.2006.3). We are grateful to Dr. D. V. Stass for his help in preparation of the manuscript. N.P.G. acknowledges the support of the Ohio Supercomputing Center.

References and Notes

- Warman, J. M.; Infelta, P. P.; de Haas, M. P.; Hummel, A. *Can. J. Chem.* **1977**, *55*, 2249–2257.
- Ametov, K. K.; Yakovlev, B. S. *High Energy Chem. (Russ.)* **1975**, *9*, 433–436.
- Sauer, M. C., Jr.; Shkrob, I. A.; Yan, J.; Schmidt, K.; Trifunac, A. D. *J. Phys. Chem.* **1996**, *100*, 11325–11335.
- Shkrob, I. A.; Sauer, M. C., Jr.; Trifunac, A. D. In *Radiation chemistry. Present studies and future trends*; Jonah, C. D., Rao, B. S. M., Eds.; Elsevier: Amsterdam, The Netherlands, 2001; pp 175–221.
- Warman, J. M.; de Haas, M. P. In *Pulse radiolysis*; Tabata, Y., Ed.; CRC Press: Boca Raton, FL, 1991; pp 101–133.
- Carrington, A.; McLachlan, A. D. *Introduction to magnetic resonance with application to chemistry and chemical physics*; Harper & Row: Publishers: New York, Evanston, London, 1967.
- Schulten, K.; Wolynes, P. G. *J. Chem. Phys.* **1978**, *68*, 3292–3297.
- Grampp, G.; Jaenicke, W. *Ber. Bunsen-Ges. Phys. Chem.* **1984**, *88*, 325–334.
- Molin, Yu. N.; Anisimov, O. A.; Grigoryants, V. M.; Molchanov, V. K.; Salikhov, K. M. *J. Phys. Chem.* **1980**, *84*, 1853–1856.
- Anisimov, O. A. In *Radical Ionic Systems*; Lund, A., Shiotani, M., Eds.; Kluwer: Dordrecht, The Netherlands, 1991; pp 285–309.
- Shkrob, I. A.; Trifunac, A. D. *J. Chem. Phys.* **1995**, *103*, 551–561.
- Melekhov, V. I.; Anisimov, O. A.; Veselov, A. V.; Molin, Yu. N. *Chem. Phys. Lett.* **1988**, *148*, 429–434.
- Salikhov, K. M.; Molin, Yu. N.; Sagdeev, R. Z.; Buchachenko, A. L. In *Spin polarization and magnetic field effects in radical reactions*; Molin, Yu. N., Ed.; Akademiai Kiado: Budapest, 1984.
- Brocklehurst, B. *Radiat. Phys. Chem.* **1997**, *50*, 213–225.
- Bagryansky, V. A.; Borovkov, V. I.; Molin, Yu. N. *Phys. Chem. Chem. Phys.* **2004**, *6*, 924–928.
- Borovkov, V. I.; Bagryansky, V. A.; Yeletskikh, I. V.; Molin, Yu. N. *Mol. Phys.* **2002**, *100*, 1379–1384.
- Anishchik, S. V.; Grigoryants, V. M.; Shebolaev, I. V.; Chernousov, Y. D.; Anisimov, O. A.; Molin, Yu. N. *Prib. Techn. Eksp. (Russ.)* **1989**, *4*, 74–79.
- Becke, A. D. *J. Chem. Phys.* **1993**, *98*, 5648–5662.
- Lee, C.; Yang, W.; Parr, R. G. *Phys. Rev. B* **1988**, *37*, 785–789.
- Frisch, M. J.; et al. *Gaussian 98*, revision A.6; Gaussian, Inc.: Pittsburgh, PA, 1998.
- Miertus, S.; Scrocco, E.; Tomasi, J. *Chem. Phys.* **1981**, *55*, 117–129.
- Cossi, M.; Barone, V.; Cammi, R.; Tomasi, J. *Chem. Phys. Lett.* **1996**, *255*, 327–335.
- Bagryansky, V. A.; Ivanov, K. L.; Borovkov, V. I.; Lukzen, N. N.; Molin, Yu. N. *J. Chem. Phys.* **2005**, *122*, 224503.
- Lozovoy, V. V.; Anishchik, S. V.; Medvedev, N. N.; Anisimov, O. A.; Molin, Yu. N. *Chem. Phys. Lett.* **1990**, *167*, 122–128.
- Wintgens, V. In *Handbook of organic photochemistry*, (v) 1; Scaiano, J. C. Ed.; CRC Press: Boca Raton, FL, 1989; pp 405–418.
- Toropov, Yu. V.; Sviridenko, F. B.; Stass, D. V.; Doktorov, A. B.; Molin, Yu. N. *Chem. Phys.* **2000**, *253*, 231–240.
- Telvin, P.; Jones, F. P.; Lafleur, S.; Trainor, L. E. H. *J. Chem. Phys.* **1986**, *85*, 4052–4055.
- Smith, G. D.; Jaffe, R. L. *Phys. Chem.* **1996**, *100*, 18718–18724.
- Behrends, R.; Kaatz, U. *J. Phys. Chem. A* **2000**, *104*, 3269–3275.
- Sceats, M. G.; Dawes, J. M. *J. Chem. Phys.* **1985**, *83*, 1298–1304.
- Klauda, J. B.; Pastor, R. W.; Brooks, B. R. *J. Phys. Chem. B* **2005**, *109*, 15684–15686.
- Lias, S. G.; Ausloos, P.; Horvath, Z. *Int. J. Chem. Kinet.* **1976**, *8*, 725–739.
- Meot-Ner (Mautner), M.; Sick, L. W.; Ausloos, P. *J. Am. Chem. Soc.* **1981**, *103*, 5342–5348.
- Ostafin, A. E.; Lipsky, S. J. *Chem. Phys.* **1993**, *98*, 5408–5418.
- Scherer, J. R.; Snyder, R. G. *J. Chem. Phys.* **1980**, *72*, 5798–5808.
- Toriyama, K.; Okazaki, M. *J. Phys. Chem.* **1992**, *96*, 6986–6991.
- Tabata, M.; Lund, A. *Radiat. Phys. Chem.* **1984**, *23*, 545–552.
- Ichikawa, T.; Shiotani, M.; Otha, N.; Katsumata, S. *J. Phys. Chem.* **1989**, *93*, 3826–3831.
- Kowalewski, J.; Liljefors, T. *Chem. Phys. Lett.* **1979**, *64*, 170–174.
- Toriyama, K. In *Radical Ionic Systems*; Lund, A., Shiotani, M., Eds.; Kluwer: Dordrecht, The Netherlands, 1991; pp 99–124.
- Adamo, C.; Barone, V.; Fortunelli, A. *J. Chem. Phys.* **1995**, *102*, 384–393.
- Importa, R.; Barone, V. *Chem. Rev.* **2004**, *104*, 1231–1253.
- Borovkov, V. I.; Velizhanin, K. A. *Chem. Phys. Lett.* **2004**, *394*, 441–445.
- Wu, J.; Nhaesi, A. H.; Asfour, A.-F. A. *J. Chem. Eng. Data* **1999**, *44*, 990–993.
- Borovkov, V. I. Unpublished results.
- Ovchinnikov, A. A.; Timashev, S. F.; Belyy, A. A. *Kinetics of diffusion controlled chemical processes*; Nova Science: Commack, NY, 1989.
- Kowert, B. A.; Sobush, K. T.; Fuqua, C. F.; Mapes, C. L.; Jones, J. B.; Zahm, J. A. *J. Phys. Chem. A* **2003**, *107*, 4790–4795.
- Closs, G. L.; Miller, J. R. *Science* **1988**, *240*, 440–447.
- Ganesan, V.; Rosokha, S. V.; Kochi, J. K. *J. Am. Chem. Soc.* **2003**, *125*, 2559–2571.
- Hostein, T. *Philos. Mag. B* **1978**, *37*, 499–526.
- Borovkov, V. I.; Ivanov, K. L.; Bagryansky, V. A.; Molin, Yu. N. *J. Phys. Chem. A* **2006**, *110*, 4622–4628.
- Stass, D. V.; Lukzen, N. N.; Tadjikov, B. M.; Grigoryants, V. M.; Molin, Yu. N. *Chem. Phys. Lett.* **1995**, *243*, 533–539.
- Shkrob, I. A.; Liu, A. D.; Sauer, M. C., Jr.; Schmidt, K. H.; Trifunac, A. D. *J. Phys. Chem. B* **1998**, *102*, 3363–3370.